Published in final edited form as:

Circulation. 2023 November 07; 148(19): 1490–1504. doi:10.1161/CIRCULATIONAHA.123.065117.

Elimination of CaMKIIδ autophosphorylation by CRISPR-Cas9 base editing improves survival and cardiac function in heart failure in mice

Simon Lebek, M.D.[1,2,3], **Xurde M. Caravia, Ph.D.**[1,2], **Francesco Chemello, Ph.D.**[1,2], **Wei Tan, M.D.**[1,2], **John R. McAnally, B.S.**[1,2], **Kenian Chen, Ph.D.**[4], **Lin Xu, Ph.D.**[4], **Ning Liu, Ph.D.**[1,2], **Rhonda Bassel-Duby, Ph.D.**[1,2], **Eric N. Olson, Ph.D.**[1,2,*]

[1]Department of Molecular Biology, University of Texas Southwestern Medical Center; Dallas, TX USA.

[2]Hamon Center for Regenerative Science and Medicine, University of Texas Southwestern Medical Center; Dallas, TX USA.

[3]Department of Internal Medicine II, University Hospital Regensburg; Regensburg, Germany.

[4]Quantitative Biomedical Research Center, Department of Population and Data Sciences, University of Texas Southwestern Medical Center; Dallas, TX USA.

Abstract

Background: Cardiovascular diseases are the main cause of worldwide morbidity and mortality, highlighting the need for new therapeutic strategies. Autophosphorylation and subsequent overactivation of the cardiac stress-responsive enzyme Ca^{2+}/calmodulin-dependent protein kinase IIδ (CaMKIIδ) serves as a central driver of multiple cardiac disorders.

Methods: To develop a comprehensive therapy for heart failure, we used CRISPR-Cas9 adenine base editing to ablate the autophosphorylation site of CaMKIIδ. We generated mice harboring a phospho-resistant CaMKIIδ mutation in the germline and subjected these mice to severe transverse aortic constriction (sTAC), a model for heart failure. Cardiac function, transcriptional changes, apoptosis, and fibrosis were assessed by echocardiography, RNA sequencing, TUNEL staining, and standard histology, respectively. Specificity toward *CaMKIIδ* gene editing was assessed using deep amplicon sequencing. Cellular Ca^{2+} homeostasis was analyzed using epifluorescence microscopy in Fura-2-loaded cardiomyocytes.

Results: Within two weeks post-sTAC surgery, 65% of all wildtype mice died and the surviving mice showed a dramatically impaired cardiac function. In contrast to wildtype mice, CaMKIIδ phospho-resistant gene-edited mice showed a mortality of only 11% and exhibited a substantially improved cardiac function post-sTAC. Moreover, CaMKIIδ phospho-resistant mice were protected from heart failure-related aberrant changes in cardiac gene expression, myocardial apoptosis, and

*Corresponding author: Eric Olson, PhD, University of Texas Southwestern Medical Center, Molecular Biology, 5323 Harry Hines Blvd., Dallas, Texas 75390-9148, Eric.Olson@utsouthwestern.edu.

Conflict of Interest Disclosures

ENO is a consultant for Vertex Pharmaceuticals, Tenaya Therapeutics, and Cardurion Pharmaceuticals. SL, RBD, and ENO are inventors on a patent application related to the content of this manuscript. All other authors have no conflict of interest.

subsequent fibrosis, which were observed in wildtype mice post-sTAC. Based on identical mouse and human genome sequences encoding the autophosphorylation site of *CaMKIIδ*, we deployed the same editing strategy to modify this pathogenic site in human induced pluripotent stem cells. Notably, we detected a >2,000-fold increased specificity for editing of *CaMKIIδ* compared to other *CaMKII* isoforms, which is an important safety feature. While wildtype cardiomyocytes showed impaired Ca^{2+} transients and an increased frequency of arrhythmias following chronic β-adrenergic stress, *CaMKIIδ*-edited cardiomyocytes were protected from these adverse responses.

Conclusions: Ablation of CaMKIIδ autophosphorylation by adenine base editing may offer a potential broad-based therapeutic concept for human cardiac disease.

Keywords

Ca^{2+}/calmodulin-dependent protein kinase IIδ; CRISPR-Cas9 gene editing; mouse model; cardioprotection; cardiac disease

Introduction

Cardiac disease represents the leading cause of worldwide morbidity and mortality with the frequency expected to increase in the future.[1,2] Despite recent advances in heart failure therapy, there remains a major need for new therapeutic strategies.[3] CRISPR-Cas9 gene editing technology is an efficient tool for human gene editing with great therapeutic potential.[4,5] Whereas conventional gene editing strategies are designed to correct specific disease-causing mutations, the frequency of specific mutations is typically very low, which precludes broad application of individual gene editing strategies.[4–6]

Ca^{2+} /calmodulin-dependent protein kinase IIδ (CaMKIIδ) is one of many CaMKII isoforms and a key regulator of cardiac physiology and signaling.[7–9] However, chronic overactivation of CaMKIIδ has been implicated in the pathophysiology of heart failure, ischemia/reperfusion injury, arrhythmias, alcoholic cardiomyopathy, myocardial hypertrophy, and sleep-disordered breathing.[10–21] Hyperactivation of cardiac CaMKIIδ has been shown to dysregulate cellular Ca^{2+} homeostasis and induce myocardial inflammation, apoptosis, and fibrosis, culminating in loss of cardiac function.[9–14,21–23] Even though there have been significant efforts to design effective CaMKIIδ inhibitors, they have not yet been successful and there is no clinical drug available for patients.[22,24,25] Thus, further optimized strategies to target CaMKIIδ are needed. CaMKII autophosphorylation at threonine-287 confers an up to 1,000-fold increased affinity for calmodulin and dramatically increases CaMKII activity by preventing association of the autoinhibitory region with the catalytic domain.[26,27] Indeed, CaMKII autophosphorylation is increased in numerous cardiac diseases and serves as a measure of total CaMKII activity.[19,20,22,28] However, up to now, it is as yet unproven whether rendering CaMKIIδ resistant to autophosphorylation confers cardioprotection. Thus, we sought to ablate the autophosphorylation site of CaMKIIδ as a potentially generalizable therapeutic concept for multiple cardiac disorders.

CRISPR-Cas9 adenine base editing (ABE) allows the conversion of adenine to guanine nucleotides. ABEs consist of a deactivated Cas9 or Cas9 nickase fused to a deoxyadenosine deaminase. When combined with appropriate single-guide RNAs (sgRNAs), ABEs can edit

adenine to guanine nucleotides within a specific window in relation to the protospacer adjacent motif (PAM) of the sgRNA.[4,6,9,29–32] Within the *CaMKIIδ* gene, threonine-287 is encoded by an ACT codon that is potentially amenable to ABE, which would create a GCT codon, thereby replacing this threonine with an alanine and consequent elimination of the autophosphorylation site of CaMKIIδ.

In the present study, we used an ABE-mediated gene editing strategy in the mouse germline to ablate the autophosphorylation site of CaMKIIδ, thereby rendering the enzyme insensitive to pathogenic hyperactivation. We show that mice with this mutation (c.A859G, p.T287A) are protected from afterload-induced heart failure. Similarly, using human cardiomyocytes derived from induced pluripotent stem cells (iPSCs), we show that this specific gene editing approach confers protection against chronic β-adrenergic stress. Our findings suggest a new strategy for maintenance of cardiac function in the settings of diverse forms of cardiac stress.

Methods

RNA-sequencing data have been uploaded and deposited at Gene Expression Omnibus (https://www.ncbi.nlm.nih.gov/geo/, accession number GSE227720). The authors declare that all other data are available within the article and its online supplementary files. An expanded methods section can be found in the Supplemental Material.

Study design and approval

The aim of the present study was to ablate the autophosphorylation site of CaMKIIδ using CRISPR-Cas9 base editing as a new therapeutic strategy against heart failure. Several sgRNAs were tested in mouse N2a cells to identify the most efficient editing approach. We found a sgRNA that is identical for the mouse and human DNA sequence and used it to generate a germline-edited c.A859G (p.T287A) mouse model that is resistant to CaMKIIδ autophosphorylation. The therapeutic effects of this amino acid mutation were evaluated in adult mice using severe transverse aortic constriction (sTAC) as a model for afterload-induced heart failure. We then applied the same CRISPR-Cas9 base editing system to human induced pluripotent stem cells (iPSCs) to test whether ablation of the autophosphorylation site of CaMKIIδ could confer cardioprotection.

We performed all experiments in replicates. Male C57BL/6 wildtype (WT) and homozygous T287A mice were randomly assigned to either sham or sTAC surgery at 10 weeks of age. Cardiac function was evaluated in each mouse one week before and one week after the surgery. Two weeks after the surgery, all mice were sacrificed. Five mice were dedicated to further molecular and three mice to histological analyses. The sample size was not predetermined by statistical tests. All samples are included in this study with no data excluded.

Animal work described in this manuscript has been approved and conducted under the oversight of the UT Southwestern Institutional Animal Care and Use Committee. Mice were housed and bred at the Animal Resource Center at the UT Southwestern Medical Center, a pathogen-free facility with a regular 12-h light/dark cycle, a temperature of 18–24° C, and a humidity of 35–60%. A maximum of 5 mice were housed in one cage with ad libitum

access to food and water, and they were monitored daily for potential health problems. Human iPSCs were previously generated and used in our laboratory.[6,9] All iPSC work was performed in compliance with the UT Southwestern Stem Cell Research Oversight Committee.

Statistical analysis

All data are reported as mean ± standard error of the mean (SEM). Shapiro-Wilk normality test was used to test for normal distribution. If a variable was not normally distributed or if the sample size was too small to assess normality, non-parametric tests were applied. Student's *t* or Mann-Whitney test were used for the comparison of two groups that were either normally or not normally distributed, respectively. Two-way ANOVA with Holm-Sidak's post-hoc correction was applied for the comparison of two genotypes (wildtype vs. T287A) that varied on intervention (sham/control vs. sTAC/ISO). Repeated measures two-way ANOVA with Holm-Sidak's post-hoc correction was used for the comparison of two genotypes (wildtype vs. T287A) with two timepoints (before acute ISO vs. after acute ISO). We refrained from performing post-hoc multiple comparisons when the two-way ANOVA was not significant. Log-rank (Mantel-Cox) test with Bonferroni's post-hoc correction was used for the comparison of survival curves. Correlations were tested by linear regression analysis and categorial data by Fisher's exact test. All statistical tests were performed using GraphPad Prism 9. We considered two-sided p-values below 0.05 statistically significant.

Results

Development of a gene editing strategy to ablate the autophosphorylation site of CaMKIIδ

Threonine-287, encoded by an ACT codon, is the autophosphorylation site of CaMKIIδ responsible for pathogenic activation of the enzyme. The adenine c.A859 is potentially editable to a guanine using ABE, which would convert the ACT to a GCT codon, resulting in replacement of threonine with alanine, thus rendering CaMKIIδ resistant to autophosphorylation (Figure 1A).

To identify an optimal ABE strategy, we tested several editing strategies in mouse N2a cells. As the optimal editing window for a specific nucleotide is often difficult to predict, we tested seven different sgRNAs (Table S1) that place *CaMKIIδ* c.A859 in protospacer positions 13–19 (with the first nucleotide immediately 5' of the PAM sequence counted as position 1). We screened different engineered deaminases, including ABEmax, an optimized narrow-windowed ABE7.10 variant,[31] and ABE8e, a wide-windowed evolved ABE7.10 variant with a 590-fold increased activity.[33] The engineered deaminase variants were fused to the engineered SpCas9 variants SpCas9-NG (targeting NG PAMs)[34] and SpRY (targeting NRN and to a lesser extent NYN PAMs).[35]

Overall, the deaminase ABE8e displayed higher c.A859G (p.T287A) editing efficiency than ABEmax (Figure 1B and Tables S1 and S2). Three sgRNAs, sgRNA2, sgRNA3, and sgRNA5, showed similar c.A859G (p.T287A) editing efficiency of ~35–39%. For subsequent studies, we selected sgRNA2 combined with ABE8e fused to SpCas9-NG, which showed a mean editing efficiency of 38.7±0.7% at adenine-16 within the targeted

genomic region (Figure 1B,C). We chose this editing strategy since sgRNA2 has complete sequence identity for mouse and human genomes. Plus, using the SpCas9-NG variant with more stringent PAM requirements was expected to have less potential off-target editing.

Using this gene editing strategy, we injected zygotes of C57BL/6 wildtype (WT) mice with sgRNA2 combined with ABE8e fused to SpCas9-NG and transferred them into the oviducts of pseudo-pregnant female mice. Genotyping of the founder F_0 litters (n=52 mice) revealed a mean c.A859G (p.T287A) editing efficiency of 59.8±4.6% (Figure 1D). We also observed base editing at adenine-18, which would create a glutamic acid to glycine substitution at residue 286 and a silent bystander edit at adenine-11. Sequencing of *CaMKIIα*, *β*, and *γ* genes revealed no editing of these *CaMKII* isoforms (Figure S1A–C). After backcrossing with C57BL/6 wildtype mice, we obtained heterozygous c.A859G (p.T287A) mice without bystander mutations that were used for further breeding. The homozygous edit was successfully transcribed into cDNA (Figure 1E).

At baseline, cardiac contractility, chamber size, and left ventricular mass were similar in WT and T287A mice with no significant differences between the groups (Figure S2). In addition, T287A mice showed ECGs similar to WT mice at baseline (Figure S3). Following acute β-adrenergic stimulation, they showed an increase in heart rate comparable to WT mice (Figure S3). When exercise capacity was evaluated by a treadmill exhaustion test, we found no significant differences between WT and T287A mice with respect to maximal velocity ($p=6.9\times10^{-1}$) or total distance ($p=6.9\times10^{-1}$) achieved on the treadmill (Figure S4A–C). All mice were subjected to transthoracic echocardiography immediately after exhaustion on the treadmill, which revealed no significant differences in cardiac function or geometry between both genotypes (Figure S4D–H). We further analyzed 1-year-old WT and T287A mice and found a similar cardiac function and geometry in both groups (Figure S5).

T287A mice are protected from afterload-induced heart failure

Male WT and phospho-resistant T287A mice at 10 weeks of age were subjected to severe transverse aortic constriction (sTAC) surgery to test whether ablation of CaMKIIδ autophosphorylation protects mice from afterload-induced heart failure (Figure 2A and Figure S6). This severe heart failure model has a high mortality rate in WT mice, which enabled subsequent survival analysis of our mice. WT mice subjected to sTAC (WT-sTAC) showed a dramatically increased mortality compared to WT-Sham mice (Figure 2B). Within the first and second week post-sTAC, 13 of 26 (50.0%) and 4 of 13 (30.8%) WT-sTAC mice died, respectively (Figure 2B). In contrast, T287A-sTAC mice were protected from heart failure-induced mortality as only one of 9 mice (11.1%) died within the two-week follow-up period (Figure 2B). Accordingly, echocardiography one-week post-sTAC showed an ~75% decrease in fractional shortening from 60.1±0.7% in WT-Sham mice to 14.3±1.5% in WT-sTAC mice ($p=8.0\times10^{-12}$) (Figure 2C,D). Importantly, T287A-sTAC mice showed improved fractional shortening of 33.9±6.5% ($p=8.7\times10^{-5}$ vs. WT-sTAC) (Figure 2D). We also observed other key features of heart failure in WT-sTAC mice, including increased left ventricular end-diastolic diameter and volume and increased left ventricular mass (Figure 2E–G). These pathological responses were significantly attenuated in T287A-sTAC mice in which CaMKIIδ was rendered phospho-resistant.

As expected, we observed a >2-fold increase in CaMKII autophosphorylation in hearts of WT-sTAC mice compared to WT-Sham mice ($p=8.6\times10^{-4}$) (Figure 2H–J). Because we ablated the autophosphorylation site of CaMKIIδ, we only detected a residual signal of autophosphorylated CaMKII in T287A mice. This low signal might either be attributable to other isoforms (e.g., CaMKIIγ) or unspecific background. Accordingly, we found substantially increased CaMKII activity in WT-sTAC mice compared to WT-Sham mice, which was reduced by 5.8-fold in T287A-sTAC mice ($p=5.6\times10^{-4}$ vs. WT-sTAC) (Figure 2K).

Mechanisms of cardioprotection conferred by *CaMKIIδ* editing

Two weeks after sTAC/sham surgery, mice were euthanized, and the hearts were harvested for histological and molecular analyses. As frequently observed in patients with critical illness, WT mice showed a significant reduction in body weight two weeks post-sTAC, which was not observed in T287A mice (Figure S7A). Macroscopically and microscopically, we observed cardiac dilation and hypertrophy in WT-sTAC mice, which was less pronounced in T287A mice following sTAC (Figure 3A–C). Accordingly, WT-sTAC mice showed significantly increased heart and lung weights compared to WT-Sham mice, further indicative of cardiac hypertrophy and heart failure (Figure S7B,C). Notably, T287A-sTAC mice were protected from both pathological alterations and their heart and lung weights were comparable to sham control mice. Additionally, we found cardiac fibrosis and myocardial infiltration of inflammatory cells in WT but not in T287A mice post-sTAC (Figure 3C and Figure S8). Quantification revealed a 1.8-fold increased area of fibrotic tissue in WT-sTAC compared to WT-Sham mice ($p=2.3\times10^{-4}$), while T287A-sTAC mice showed low levels of fibrosis ($p=1.9\times10^{-4}$ vs. WT-sTAC) (Figure S8B). In accordance with myocardial fibrosis, we detected substantially increased apoptosis in WT but not in T287A mice post-sTAC (Figure 3D,E). Compared to WT-Sham mice, we found a 15.7-fold increased percentage of apoptotic cells in WT-sTAC mice ($p=2.6\times10^{-5}$) (Figure 3E). In contrast, T287A-sTAC mice showed only a slight and non-significant increase in apoptotic cells compared to T287A-Sham mice (Figure 3E).

We then performed RNA sequencing of whole hearts to investigate transcriptomic changes. Principal component analysis (PCA) revealed three distinct transcriptomic profiles. While both WT and T287A sham-treated mice were similar, WT mice subjected to sTAC showed a substantially different cardiac transcriptome (Figure 4A). Importantly, T287A mice subjected to sTAC formed a third transcriptomic cluster that was closer to the healthy sham control mice than to WT-sTAC mice (Figure 4A). In WT mice, we found a total of 5,994 genes differentially expressed two weeks after sTAC (3,171 genes up- and 2,823 genes downregulated in WT-sTAC vs. WT-Sham). Compared to WT-sTAC, there were 3,787 differentially expressed genes in T287A-sTAC hearts (1,787 genes up- and 2,000 genes downregulated in T287A-sTAC). For the subsequent analysis of highly enriched gene sets, we only considered at least 2-fold differentially expressed genes (Figure 4B). Gene Ontology analysis of the 1,381 highly upregulated genes in WT-sTAC compared to WT-Sham hearts revealed pathways related to pathological remodeling and inflammation (Figure 4C,D). Additionally, the 601 substantially (fold-change >2) downregulated genes in WT-sTAC hearts were mainly linked to cardiac performance and

metabolism (Figure 4C,E). Importantly, rendering CaMKIIδ phospho-resistant protected hearts from these pathological transcriptomic changes. Compared to WT-sTAC mice, the 264 highly upregulated (fold-change >2) genes in T287A-sTAC hearts were mainly linked to cardiac function, performance, and metabolism (Figure 4F,G). In contrast, the 496 genes that were substantially (fold-change >2) downregulated in T287A-sTAC vs. WT-sTAC hearts were mainly related to cardiac remodeling and inflammation (Figure 4F,H).

Editing efficiency and analysis of potential off-target DNA editing in human iPSCs

We next tested whether our editing approach was also feasible in the human genome and could thus potentially be therapeutically applicable. Therefore, human iPSCs were nucleofected with sgRNA2 and ABE8e fused to SpCas9-NG. This revealed a similar editing pattern as observed in the mouse genome with a mean c.A859G (p.T287A) editing efficiency of 48.4±1.0% (Figure 5A). Since other CaMKII isoforms are highly expressed in several organs other than the heart, where they are involved in important processes such as brain and skeletal muscle function, specificity of the gene editing approach for the *CaMKIIδ* isoform is important.[16,17,36] Notably, we observed no significant editing of any other *CaMKII* isoforms, as determined by deep amplicon sequencing (Figure 5B–E). We found a ~2306-, ~3267-, ~2254-fold increased c.A859G (p.T287A) editing efficiency for *CaMKIIδ* compared to *CaMKIIα*, *β*, and *γ*, respectively (Figure 5F).

Furthermore, we analyzed the top 8 predicted genomic sites for potential off-target editing, as predicted by the bioinformatic tool CRISPOR (Figure 5B and Tables S3 and S4).[37] We detected minimal to no off-target editing (less than 1.2%) at any adenines within the top 8 predicted off-target sites (Figure 5G). None of these sites represents a coding region in the genome, making even minimal off-target editing of these sites less likely to be detrimental.

ABE-treated iPSC-CMs are protected from chronic β-adrenergic stress

To test whether treatment with sgRNA2 and ABE8e fused to SpCas9-NG confers cardioprotection in human cardiomyocytes, we established an iPSC-line using the same ABE strategy as in mice (Figure 5A) and differentiated them into cardiomyocytes (iPSC-CMs). Sequencing of the cDNA revealed successful transcription of the editing pattern of sgRNA2 (homozygous for c.A859G (p.T287A) and heterozygous for both c.A857G (p.E286G) and c.A864G (p.V288V)) (Figure 6A). Notably, T287A iPSC-CMs were still responsive to acute β-adrenergic stimulation (Figure S9).

To test for potential cardioprotection, WT and T287A iPSC-CMs were treated with either normal control medium or with 100 nM isoproterenol for 10 days (ISO) to mimic chronic β-adrenergic stress as it occurs in heart failure. As anticipated, Western blot analyses revealed a 2.9-fold increase in autophosphorylated CaMKII in WT iPSC-CMs upon chronic treatment with ISO (0.60±0.18) compared to control (0.21±0.05, $p=8.9\times10^{-3}$) (Figure 6B–D). In T287A-edited iPSC-CMs, ISO treatment did not increase the level of CaMKII autophosphorylation and only minimal autophosphorylation signal was detected. This residual signal may result from non-edited CaMKIIγ (which is also expressed in cardiomyocytes) or unspecific background. In accordance with an expected increase in CaMKII autophosphorylation with ISO treatment, CaMKII activity increased from (in

nmol/min/mg) 4.8±0.5 in WT-Control iPSC-CMs to 12.5±3.8 upon treatment with ISO ($p=1.2\times10^{-2}$, Figure 6E). Compared to WT iPSC-CMs, the T287A iPSC-CMs showed a 4.3-fold lower CaMKII activity upon ISO stimulation ($p=5.5\times10^{-3}$) (Figure 6E).

Stimulated Ca^{2+} transients were measured to assess cellular Ca^{2+} homeostasis in WT and T287A iPSC-CMs upon control and chronic ISO treatment (Figure 6F). We detected no differences in diastolic Ca^{2+} levels (Figure 6G). However, chronic ISO treatment decreased Ca^{2+} transient amplitude from (in $\Delta F_{340}/F_{380}$) 0.55±0.03 to 0.37±0.03 in WT iPSC-CMs ($p=2.0\times10^{-5}$) (Figure 6H). Compared to WT iPSC-CMs, the T287A iPSC-CMs showed an increased Ca^{2+} transient amplitude of 0.75±0.03 upon control conditions ($p=1.4\times10^{-6}$ vs. WT-Control) and were resistant to ISO-induced deterioration of cellular Ca^{2+} homeostasis. Similarly, relaxation times to both 50% and 80% of diastolic Ca^{2+} levels were decreased in WT-ISO iPSC-CMs but not in T287A-ISO iPSC-CMs (Figure 6I,J). ISO treatment of WT iPSC-CMs increased the risk for arrhythmias by ~7.2-fold, resulting in 68.4% of iPSC-CMs showing arrhythmias ($p=2.0\times10^{-4}$) (Figure 6K). The proarrhythmic risk upon ISO treatment was reduced by ~6.5-fold when CaMKIIδ was rendered phospho-resistant ($p=6.3\times10^{-4}$ for T287A-ISO vs. WT-ISO).

Analyses of Ca^{2+} characteristics after paused electrical stimulation have previously been used to estimate diastolic sarcoplasmic reticulum Ca^{2+} leak, a key feature of cardiac dysfunction.[12,22] After 10 s of paused stimulation, we found increased cytosolic Ca^{2+} overload in WT iPSC-CMs upon chronic ISO ($p=5.3\times10^{-6}$ vs. WT-Control), but not when the CaMKIIδ autophosphorylation site was ablated (Figure S10A,B). This cytosolic Ca^{2+} overload indicates that there might be less Ca^{2+} in the sarcoplasmic reticulum and thus less Ca^{2+} available for the next contraction.[10,12,19,22] Indeed, the gain of post-pause Ca^{2+} transient amplitude was impaired by ~1.9-fold in WT iPSC-CMs upon chronic ISO compared to control iPSC-CMs ($p=8.6\times10^{-6}$) (Figure S10C). Upon control conditions, T287A iPSC-CMs showed an increased gain of post-pause Ca^{2+} transient amplitude compared to WT ($p=8.4\times10^{-3}$), which was resistant to ISO-induced impairment (Figure S10C). The post-pause cytosolic Ca^{2+} overload correlated significantly negative with the gain of post-pause Ca^{2+} transient amplitude (Figure S10D,E). Moreover, we also found a negative correlation between the post-pause cytosolic Ca^{2+} overload and the stimulated steady-state Ca^{2+} transient amplitude (Figure S10F,G), further validating our experimental approach. Interestingly, there was a clear separation between control- and chronic ISO-treatment only in WT but not in T287A iPSC-CMs, further indicating that ablating CaMKIIδ autophosphorylation renders cardiomyocytes resistant to chronic β-adrenergic stress.

Discussion

In the present study, we screened several sgRNAs and ABEs to identify an optimal base editing strategy capable of rendering mouse and human CaMKIIδ resistant to autophosphorylation. Using this cross-species editing strategy, we created a mouse model lacking the autophosphorylation site of CaMKIIδ, which conferred cardioprotection against afterload-induced heart failure following sTAC, resulting in improved survival. Additionally,

we showed that *CaMKIIδ*-edited human iPSC-CMs were protected against chronic β-adrenergic stress.

CRISPR-Cas9 base editing can precisely convert one nucleotide to another without inducing DNA double-stranded breaks.[4,6,29–31,38] To date, most gene editing strategies have been designed to correct monogenic disease-causing mutations.[4,6,32,33,39–42] However, the frequency of these mutations is typically low, which prevents broad application of this strategy. The autophosphorylation site of CaMKIIδ represents a promising therapeutic target for a wide range of cardiovascular disorders and base editing can be used to ablate this critical site. The concept of blocking pathogenic signaling by CRISPR-Cas9 gene editing could also be extended to other human diseases with other pathomechanisms.

CaMKIIδ is a key regulator of cardiac function and signaling, while chronic overactivation promotes cardiac disease and dysfunction.[7,8,10–20] The enzyme consists of three domains, namely the catalytic, regulatory, and association domains.[7] Ca^{2+}/calmodulin binding to the regulatory domain induces a conformational change, which exposes the catalytic domain and activates the enzyme.[7] Besides Ca^{2+}/calmodulin binding, CaMKIIδ is also subject to posttranslational modification of several amino acids in the regulatory domain. Autophosphorylation of threonine-287,[26,27] oxidation of methionine-281 and methionine-282 by reactive oxygen species,[43] O-linked N-acetylglucosaminylation of serine-280 during hyperglycemia,[44,45] and nitrosylation of cysteine-290 through nitric oxide-dependent signaling[46] have been identified. Posttranslational modification of these amino acid residues prevents re-association of the autoinhibitory region with the catalytic domain resulting in sustained CaMKII hyperactivation and cardiac disease. The functional relevance and importance of each individual posttranslational modification site compared with the other sites remains to be determined. CaMKII autophosphorylation of threonine-287 has been linked to several cardiac diseases and has been used as a measure of total CaMKII activity.[19,20,22,26–28] However, the impact of genetic ablation of the autophosphorylation site of CaMKIIδ on cardiac function has not yet been explored. Analyzing a phospho-resistant CaMKIIδ mouse model allows deeper insights into the mechanisms of CaMKIIδ-dependent signaling in cardiac disease. Previous studies showed a correlative association between CaMKIIδ autophosphorylation and cardiac disorders. Here, we analyzed a phospho-resistant CaMKIIδ mouse model and provide direct evidence for the role of CaMKIIδ-dependent signaling in heart disease.[19,20,22,28] Our findings show that mice harboring a phospho-resistant CaMKIIδ display improved survival and cardiac function in heart failure.

It has previously been shown that autophosphorylation increases the binding affinity of CaMKIIδ for calmodulin and slows calmodulin dissociation from CaMKIIδ in isolated rabbit cardiomyocytes following adenoviral transduction of either WT, phospho-mimetic (T287D) or phospho-resistant (T287A) CaMKIIδ.[27] Intracardiac injection of adeno-associated virus serotype 9 expressing the CaMKIIδ T287A mutant was found to attenuate myocardial injury after ischemia/reperfusion in rats.[47] However, viral overexpression only resulted in ~60–125% expression over the endogenous CaMKIIδ.[27,47] This indicates the existence of a mixed population retaining ~31–63% WT CaMKIIδ. Additionally, CaMKII overexpression itself promotes cardiac disease, making these studies difficult to

interpret.[48,49] We show that complete ablation of the CaMKIIδ autophosphorylation site in mice prevents pathogenic activation of the enzyme, but does not affect overall CaMKII expression nor does this mutation have adverse consequences.

As enhanced CaMKIIδ signaling is an established driver of cardiac disease, CaMKIIδ inhibition has been identified as a promising therapeutic target.[16,17,22,50,51] However, to date, there are no clinically available enzyme inhibitors.[16] KN93, a small-molecule allosteric inhibitor, has been extensively studied and shown to improve cardiac function in different disease models.[16,17] However, the usefulness of KN93 is limited by relatively low potency and off-target effects on a number of ion channels, such as potassium channels.[52] Other compounds, like autocamtide-2 related inhibitory peptide, have poor bioavailability and ATP-competitive inhibitors also inhibit other kinases.[16,17] Hesperadin, an ATP-competitive CaMKII inhibitor, targets both CaMKIIδ and Aurora B kinase, conferring cardioprotection and antitumor effects.[53] Two other ATP-competitive CaMKII inhibitors, RA608 and RA306, have recently been demonstrated to improve cardiac function *in vivo* upon afterload-induced heart failure and in a mouse model of dilated cardiomyopathy, respectively.[24,25] However, the IC_{50} of both compounds for CaMKIIδ was only 4–6-fold lower than for CaMKIIα, ~0.5-fold compared to CaMKIIγ, and RA608 showed 70% inhibition of CaMKIIβ.[24,25] The lack of CaMKIIδ isoform specificity represents a major challenge in the development of CaMKII inhibitors.[16,17] While CaMKIIα and β are highly expressed in the brain, where they are critically involved in learning and memory, CaMKIIγ has been linked to exercise performance in skeletal muscle.[16,17,36] This highlights the necessity of specifically targeting CaMKIIδ, which is the main CaMKII isoform involved cardiac pathology.[10–21]

We recently developed a CRISPR-Cas9 gene editing strategy to ablate the oxidative activation sites of CaMKIIδ.[9] We found that rendering CaMKIIδ resistant to oxidative activation represents a promising therapeutic strategy to ameliorate direct consequences of oxidative stress (as in ischemia/reperfusion injury).[9] In addition to oxidation, autophosphorylation is a major activator of CaMKIIδ and has been shown to promote various cardiac disorders. Future work that compares targeting the different posttranslational modification sites of CaMKIIδ will help to identify the most comprehensive and beneficial therapeutic approach. Therefore, in the present study, we have developed a new ABE strategy to genetically ablate the autophosphorylation site of CaMKIIδ. The optimal sgRNA identified in this study showed ~2306-, ~3267-, and ~2254-fold specificity for c.A859G (p.T287A) editing of *CaMKIIδ* compared to *CaMKIIα*, *β*, and *γ*, respectively. This sgRNA specificity is higher than our previously reported gene editing strategy for the oxidative activation sites of CaMKIIδ, which represents an important safety feature.[9] Moreover, here we present a concept that improves survival in heart failure. Rendering CaMKIIδ resistant to autophosphorylation might be applicable to a broader range of cardiac diseases than ablating the oxidative activation sites, but this remains to be tested. Notably, using CRISPR-Cas9 gene editing to ablate the autophosphorylation site of CaMKIIδ only prevents pathological overactivation and does not block basal enzyme activity. Since the Ca^{2+}/calmodulin binding site is not targeted, CaMKIIδ can still exert its physiological function as a cellular Ca^{2+} sensor. Moreover, we detected no off-target editing within a coding region of the top 8 predicted genomic sites for potential off-target editing, reducing the risk of potential adverse side effects.

Permanent modification of an otherwise normal gene also raises questions from an ethical perspective. One may argue that this approach can be justified when traditional and currently available therapeutic strategies are ineffective or not well-tolerated. Permanent modification of a specific pathogenic signaling cascade may be justified especially for chronic disorders (e.g., chronic heart failure), where permanent perturbation of a pathomechanism is sustained for many years causing organ failure. It will be imperative to carefully assess safety to understand the long-term consequences of the editing strategy, as such a modification would be permanent. In our study, we did not detect overt adverse effects in the basal phenotype of mice harboring the T287A mutation. In the context of personalized medicine, it will be critical to identify the optimal gene to edit for each group of patients, which depends on the predominant pathomechanism of each disease, the editability of the respective genes, and their other functions that might not necessarily be related to pathology. For multimorbid patients, simultaneous approaches targeting different pathomechanisms could also be considered.

A significant limitation of our study is that we performed gene editing in the germline, which is not acceptable clinically or ethically. Thus, it will be important to test whether ablating CaMKIIδ autophosphorylation is also feasible postnatally and whether it could also reverse or prevent disease progression after its onset (e.g., in human iPSC-CMs after chronic β-adrenergic stress or in mice when early heart failure has already been developed). Delivery of the CRISPR-Cas9 base editing components into heart cells could be achieved with methods used in gene therapy approaches (e.g., using cardiotropic adeno-associated viruses), which have been shown to enable high editing efficiency *in vivo*.[6,9] Efficiency of delivery is another important factor, as the number of cells expressing the gene editing components would limit the overall treatment success. These aspects are the next steps of investigation required to further develop elimination of CaMKIIδ autophosphorylation as a potential broad-based therapeutic concept for human cardiac disease.

Supplementary Material

Refer to Web version on PubMed Central for supplementary material.

Acknowledgments

We acknowledge Dr. Andreas Chai and all other members of the Olson laboratory for constructive advice; Dr. Damir Alzhanov for technical assistance; Jose Cabrera for graphics; Drs. Jian Xu and Yoon J. Kim from the Children's Research Institute for Illumina NextSeq sequencing; John Shelton from the Molecular Histopathology Core for helping with histology; the UTSW McDermott Center Sanger Sequencing Core; and the UTSW McDermott Center Next Generation Sequencing Core.

Sources of Funding

This study was funded by grants from the National Institutes of Health (R01HL130253, R01HL157281, P50HD087351; all to ENO and RBD), the Fondation Leducq Transatlantic Network of Excellence (to ENO), the Robert A. Welch Foundation (1–0025; to ENO), the British Heart Foundation's Big Beat Challenge award to CureHeart (BBC/F/21/220106; to ENO), the German Research Foundation (DFG, LE 5009/1–1; to SL), the German Cardiac Society (to SL), and the American Heart Association (AHA, 23POST1026194; to XMC).

Non-standard Abbreviations and Acronyms

ABE	adenine base editing
CaMKIIδ	Ca^{2+}/calmodulin-dependent protein kinase IIδ
Cas9	CRISPR-associated protein 9
CRISPR	clustered regularly interspaced short palindromic repeats
iPSC	induced pluripotent stem cell
iPSC-CM	iPSC-derived cardiomyocyte
ISO	isoproterenol
PAM	protospacer adjacent motif
sgRNA	single-guide RNA
SpCas9	*Streptococcus pyogenes* Cas9
sTAC	severe transverse aortic constriction
T287A	phospho-resistant CaMKIIδ
WT	wildtype

References

1. Virani SS, Alonso A, Aparicio HJ, Benjamin EJ, Bittencourt MS, Callaway CW, Carson AP, Chamberlain AM, Cheng S, Delling FN, et al. Heart Disease and Stroke Statistics-2021 Update: A Report From the American Heart Association. Circulation. 2021;143:e254–e743. doi: 10.1161/CIR.0000000000000950 [PubMed: 33501848]
2. Collaborators GBDRF. Global burden of 87 risk factors in 204 countries and territories, 1990–2019: a systematic analysis for the Global Burden of Disease Study 2019. Lancet. 2020;396:1223–1249. doi: 10.1016/S0140-6736(20)30752-2 [PubMed: 33069327]
3. Heidenreich PA, Bozkurt B, Aguilar D, Allen LA, Byun JJ, Colvin MM, Deswal A, Drazner MH, Dunlay SM, Evers LR, et al. 2022 AHA/ACC/HFSA Guideline for the Management of Heart Failure: A Report of the American College of Cardiology/American Heart Association Joint Committee on Clinical Practice Guidelines. Circulation. 2022;145:e895–e1032. doi: 10.1161/CIR.0000000000001063 [PubMed: 35363499]
4. Liu N, Olson EN. CRISPR Modeling and Correction of Cardiovascular Disease. Circ Res. 2022;130:1827–1850. doi: 10.1161/CIRCRESAHA.122.320496 [PubMed: 35679361]
5. Nishiyama T, Zhang Y, Cui M, Li H, Sanchez-Ortiz E, McAnally JR, Tan W, Kim J, Chen K, Xu L, et al. Precise genomic editing of pathogenic mutations in RBM20 rescues dilated cardiomyopathy. Sci Transl Med. 2022;14:eade1633. doi: 10.1126/scitranslmed.ade1633 [PubMed: 36417486]
6. Chemello F, Chai AC, Li H, Rodriguez-Caycedo C, Sanchez-Ortiz E, Atmanli A, Mireault AA, Liu N, Bassel-Duby R, Olson EN. Precise correction of Duchenne muscular dystrophy exon deletion mutations by base and prime editing. Sci Adv. 2021;7. doi: 10.1126/sciadv.abg4910
7. Beckendorf J, van den Hoogenhof MMG, Backs J. Physiological and unappreciated roles of CaMKII in the heart. Basic Res Cardiol. 2018;113:29. doi: 10.1007/s00395-018-0688-8 [PubMed: 29905892]
8. Maier LS. Role of CaMKII for signaling and regulation in the heart. Front Biosci (Landmark Ed). 2009;14:486–496. doi: 10.2741/3257 [PubMed: 19273080]

9. Lebek S, Chemello F, Caravia XM, Tan W, Li H, Chen K, Xu L, Liu N, Bassel-Duby R, Olson EN. Ablation of CaMKIIδ oxidation by CRISPR-Cas9 base editing as a therapy for cardiac disease. Science. 2023;379:179–185. doi: 10.1126/science.ade1105 [PubMed: 36634166]
10. Neef S, Dybkova N, Sossalla S, Ort KR, Fluschnik N, Neumann K, Seipelt R, Schondube FA, Hasenfuss G, Maier LS. CaMKII-dependent diastolic SR Ca2+ leak and elevated diastolic Ca2+ levels in right atrial myocardium of patients with atrial fibrillation. Circ Res. 2010;106:1134–1144. doi: 10.1161/CIRCRESAHA.109.203836 [PubMed: 20056922]
11. Backs J, Backs T, Neef S, Kreusser MM, Lehmann LH, Patrick DM, Grueter CE, Qi X, Richardson JA, Hill JA, et al. The delta isoform of CaM kinase II is required for pathological cardiac hypertrophy and remodeling after pressure overload. Proc Natl Acad Sci U S A. 2009;106:2342–2347. doi: 10.1073/pnas.0813013106 [PubMed: 19179290]
12. Lebek S, Pichler K, Reuthner K, Trum M, Tafelmeier M, Mustroph J, Camboni D, Rupprecht L, Schmid C, Maier LS, et al. Enhanced CaMKII-Dependent Late INa Induces Atrial Proarrhythmic Activity in Patients With Sleep-Disordered Breathing. Circ Res. 2020;126:603–615. doi: 10.1161/CIRCRESAHA.119.315755 [PubMed: 31902278]
13. Zhang T, Brown JH. Role of Ca2+/calmodulin-dependent protein kinase II in cardiac hypertrophy and heart failure. Cardiovasc Res. 2004;63:476–486. doi: 10.1016/j.cardiores.2004.04.026 [PubMed: 15276473]
14. Ling H, Gray CB, Zambon AC, Grimm M, Gu Y, Dalton N, Purcell NH, Peterson K, Brown JH. Ca2+/Calmodulin-dependent protein kinase II delta mediates myocardial ischemia/reperfusion injury through nuclear factor-kappaB. Circ Res. 2013;112:935–944. doi: 10.1161/CIRCRESAHA.112.276915 [PubMed: 23388157]
15. Luo M, Guan X, Luczak ED, Lang D, Kutschke W, Gao Z, Yang J, Glynn P, Sossalla S, Swaminathan PD, et al. Diabetes increases mortality after myocardial infarction by oxidizing CaMKII. J Clin Invest. 2013;123:1262–1274. doi: 10.1172/JCI65268 [PubMed: 23426181]
16. Nassal D, Gratz D, Hund TJ. Challenges and Opportunities for Therapeutic Targeting of Calmodulin Kinase II in Heart. Front Pharmacol. 2020;11:35. doi: 10.3389/fphar.2020.00035 [PubMed: 32116711]
17. Pellicena P, Schulman H. CaMKII inhibitors: from research tools to therapeutic agents. Front Pharmacol. 2014;5:21. doi: 10.3389/fphar.2014.00021 [PubMed: 24600394]
18. Mustroph J, Wagemann O, Lebek S, Tarnowski D, Ackermann J, Drzymalski M, Pabel S, Schmid C, Wagner S, Sossalla S, et al. SR Ca(2+)-leak and disordered excitation-contraction coupling as the basis for arrhythmogenic and negative inotropic effects of acute ethanol exposure. J Mol Cell Cardiol. 2018;116:81–90. doi: 10.1016/j.yjmcc.2018.02.002 [PubMed: 29410242]
19. Fischer TH, Eiringhaus J, Dybkova N, Forster A, Herting J, Kleinwachter A, Ljubojevic S, Schmitto JD, Streckfuss-Bomeke K, Renner A, et al. Ca(2+) /calmodulin-dependent protein kinase II equally induces sarcoplasmic reticulum Ca(2+) leak in human ischaemic and dilated cardiomyopathy. Eur J Heart Fail. 2014;16:1292–1300. doi: 10.1002/ejhf.163 [PubMed: 25201344]
20. Toischer K, Rokita AG, Unsold B, Zhu W, Kararigas G, Sossalla S, Reuter SP, Becker A, Teucher N, Seidler T, et al. Differential cardiac remodeling in preload versus afterload. Circulation. 2010;122:993–1003. doi: 10.1161/CIRCULATIONAHA.110.943431 [PubMed: 20733099]
21. Lebek S, Wester M, Pec J, Poschenrieder F, Tafelmeier M, Fisser C, Provaznik Z, Schopka S, Debl K, Schmid C, et al. Abnormal P-wave terminal force in lead V1 is a marker for atrial electrical dysfunction but not structural remodelling. ESC Heart Fail. 2021;8:4055–4066. doi: 10.1002/ehf2.13488 [PubMed: 34196135]
22. Lebek S, Plossl A, Baier M, Mustroph J, Tarnowski D, Lucht CM, Schopka S, Florchinger B, Schmid C, Zausig Y, et al. The novel CaMKII inhibitor GS-680 reduces diastolic SR Ca leak and prevents CaMKII-dependent pro-arrhythmic activity. J Mol Cell Cardiol. 2018;118:159–168. doi: 10.1016/j.yjmcc.2018.03.020 [PubMed: 29614261]
23. Pabel S, Knierim M, Stehle T, Alebrand F, Paulus M, Sieme M, Herwig M, Barsch F, Kortl T, Poppl A, et al. Effects of Atrial Fibrillation on the Human Ventricle. Circ Res. 2022;130:994–1010. doi: 10.1161/CIRCRESAHA.121.319718 [PubMed: 35193397]
24. Mustroph J, Drzymalski M, Baier M, Pabel S, Biedermann A, Memmel B, Durczok M, Neef S, Sag CM, Floerchinger B, et al. The oral Ca/calmodulin-dependent kinase II inhibitor

RA608 improves contractile function and prevents arrhythmias in heart failure. ESC Heart Fail. 2020;7:2871–2883. doi: 10.1002/ehf2.12895 [PubMed: 32691522]

25. Beauverger P, Ozoux ML, Begis G, Glenat V, Briand V, Philippo MC, Daveu C, Tavares G, Roy S, Corbier A, et al. Reversion of cardiac dysfunction by a novel orally available calcium/calmodulin-dependent protein kinase II inhibitor, RA306, in a genetic model of dilated cardiomyopathy. Cardiovasc Res. 2020;116:329–338. doi: 10.1093/cvr/cvz097 [PubMed: 31038167]
26. Meyer T, Hanson PI, Stryer L, Schulman H. Calmodulin trapping by calcium-calmodulin-dependent protein kinase. Science. 1992;256:1199–1202. doi: 10.1126/science.256.5060.1199 [PubMed: 1317063]
27. Simon M, Ko CY, Rebbeck RT, Baidar S, Cornea RL, Bers DM. CaMKIIdelta post-translational modifications increase affinity for calmodulin inside cardiac ventricular myocytes. J Mol Cell Cardiol. 2021;161:53–61. doi: 10.1016/j.yjmcc.2021.08.002 [PubMed: 34371035]
28. Ljubojevic-Holzer S, Herren AW, Djalinac N, Voglhuber J, Morotti S, Holzer M, Wood BM, Abdellatif M, Matzer I, Sacherer M, et al. CaMKIIdeltaC Drives Early Adaptive Ca(2+) Change and Late Eccentric Cardiac Hypertrophy. Circ Res. 2020;127:1159–1178. doi: 10.1161/CIRCRESAHA.120.316947 [PubMed: 32821022]
29. Gaudelli NM, Komor AC, Rees HA, Packer MS, Badran AH, Bryson DI, Liu DR. Programmable base editing of A*T to G*C in genomic DNA without DNA cleavage. Nature. 2017;551:464–471. doi: 10.1038/nature24644 [PubMed: 29160308]
30. Komor AC, Kim YB, Packer MS, Zuris JA, Liu DR. Programmable editing of a target base in genomic DNA without double-stranded DNA cleavage. Nature. 2016;533:420–424. doi: 10.1038/nature17946 [PubMed: 27096365]
31. Koblan LW, Doman JL, Wilson C, Levy JM, Tay T, Newby GA, Maianti JP, Raguram A, Liu DR. Improving cytidine and adenine base editors by expression optimization and ancestral reconstruction. Nat Biotechnol. 2018;36:843–846. doi: 10.1038/nbt.4172 [PubMed: 29813047]
32. Chai AC, Cui M, Chemello F, Li H, Chen K, Tan W, Atmanli A, McAnally JR, Zhang Y, Xu L, et al. Base editing correction of hypertrophic cardiomyopathy in human cardiomyocytes and humanized mice. Nat Med. 2023;29:401–411. doi: 10.1038/s41591-022-02176-5 [PubMed: 36797478]
33. Richter MF, Zhao KT, Eton E, Lapinaite A, Newby GA, Thuronyi BW, Wilson C, Koblan LW, Zeng J, Bauer DE, et al. Phage-assisted evolution of an adenine base editor with improved Cas domain compatibility and activity. Nat Biotechnol. 2020;38:883–891. doi: 10.1038/s41587-020-0453-z [PubMed: 32433547]
34. Nishimasu H, Shi X, Ishiguro S, Gao L, Hirano S, Okazaki S, Noda T, Abudayyeh OO, Gootenberg JS, Mori H, et al. Engineered CRISPR-Cas9 nuclease with expanded targeting space. Science. 2018;361:1259–1262. doi: 10.1126/science.aas9129 [PubMed: 30166441]
35. Walton RT, Christie KA, Whittaker MN, Kleinstiver BP. Unconstrained genome targeting with near-PAMless engineered CRISPR-Cas9 variants. Science. 2020;368:290–296. doi: 10.1126/science.aba8853 [PubMed: 32217751]
36. Wang Q, Hernandez-Ochoa EO, Viswanathan MC, Blum ID, Do DC, Granger JM, Murphy KR, Wei AC, Aja S, Liu N, et al. CaMKII oxidation is a critical performance/disease trade-off acquired at the dawn of vertebrate evolution. Nat Commun. 2021;12:3175. doi: 10.1038/s41467-021-23549-3 [PubMed: 34039988]
37. Concordet JP, Haeussler M. CRISPOR: intuitive guide selection for CRISPR/Cas9 genome editing experiments and screens. Nucleic Acids Res. 2018;46:W242–W245. doi: 10.1093/nar/gky354 [PubMed: 29762716]
38. Olson EN. Toward the correction of muscular dystrophy by gene editing. Proc Natl Acad Sci U S A. 2021;118. doi: 10.1073/pnas.2004840117
39. Amoasii L, Hildyard JCW, Li H, Sanchez-Ortiz E, Mireault A, Caballero D, Harron R, Stathopoulou TR, Massey C, Shelton JM, et al. Gene editing restores dystrophin expression in a canine model of Duchenne muscular dystrophy. Science. 2018;362:86–91. doi: 10.1126/science.aau1549 [PubMed: 30166439]
40. Amoasii L, Li H, Zhang Y, Min YL, Sanchez-Ortiz E, Shelton JM, Long C, Mireault AA, Bhattacharyya S, McAnally JR, et al. In vivo non-invasive monitoring of dystrophin correction in

a new Duchenne muscular dystrophy reporter mouse. Nat Commun. 2019;10:4537. doi: 10.1038/s41467-019-12335-x [PubMed: 31586095]

41. Koblan LW, Erdos MR, Wilson C, Cabral WA, Levy JM, Xiong ZM, Tavarez UL, Davison LM, Gete YG, Mao X, et al. In vivo base editing rescues Hutchinson-Gilford progeria syndrome in mice. Nature. 2021;589:608–614. doi: 10.1038/s41586-020-03086-7 [PubMed: 33408413]
42. Atmanli A, Chai AC, Cui M, Wang Z, Nishiyama T, Bassel-Duby R, Olson EN. Cardiac Myoediting Attenuates Cardiac Abnormalities in Human and Mouse Models of Duchenne Muscular Dystrophy. Circ Res. 2021;129:602–616. doi: 10.1161/CIRCRESAHA.121.319579 [PubMed: 34372664]
43. Erickson JR, Joiner ML, Guan X, Kutschke W, Yang J, Oddis CV, Bartlett RK, Lowe JS, O'Donnell SE, Aykin-Burns N, et al. A dynamic pathway for calcium-independent activation of CaMKII by methionine oxidation. Cell. 2008;133:462–474. doi: 10.1016/j.cell.2008.02.048 [PubMed: 18455987]
44. Hegyi B, Fasoli A, Ko CY, Van BW, Alim CC, Shen EY, Ciccozzi MM, Tapa S, Ripplinger CM, Erickson JR, et al. CaMKII Serine 280 O-GlcNAcylation Links Diabetic Hyperglycemia to Proarrhythmia. Circ Res. 2021;129:98–113. doi: 10.1161/CIRCRESAHA.120.318402 [PubMed: 33926209]
45. Erickson JR, Pereira L, Wang L, Han G, Ferguson A, Dao K, Copeland RJ, Despa F, Hart GW, Ripplinger CM, et al. Diabetic hyperglycaemia activates CaMKII and arrhythmias by O-linked glycosylation. Nature. 2013;502:372–376. doi: 10.1038/nature12537 [PubMed: 24077098]
46. Erickson JR, Nichols CB, Uchinoumi H, Stein ML, Bossuyt J, Bers DM. S-Nitrosylation Induces Both Autonomous Activation and Inhibition of Calcium/Calmodulin-dependent Protein Kinase II delta. J Biol Chem. 2015;290:25646–25656. doi: 10.1074/jbc.M115.650234 [PubMed: 26316536]
47. Lu HT, Feng RQ, Tang JK, Zhou JJ, Gao F, Ren J. CaMKII/calpain interaction mediates ischemia/reperfusion injury in isolated rat hearts. Cell Death Dis. 2020;11:388. doi: 10.1038/s41419-020-2605-y [PubMed: 32439852]
48. Maier LS, Zhang T, Chen L, DeSantiago J, Brown JH, Bers DM. Transgenic CaMKIIdeltaC overexpression uniquely alters cardiac myocyte Ca2+ handling: reduced SR Ca2+ load and activated SR Ca2+ release. Circ Res. 2003;92:904–911. doi: 10.1161/01.RES.0000069685.20258.F1 [PubMed: 12676813]
49. Zhang T, Maier LS, Dalton ND, Miyamoto S, Ross J, Jr., Bers DM, Brown JH. The deltaC isoform of CaMKII is activated in cardiac hypertrophy and induces dilated cardiomyopathy and heart failure. Circ Res. 2003;92:912–919. doi: 10.1161/01.RES.0000069686.31472.C5 [PubMed: 12676814]
50. Neef S, Steffens A, Pellicena P, Mustroph J, Lebek S, Ort KR, Schulman H, Maier LS. Improvement of cardiomyocyte function by a novel pyrimidine-based CaMKII-inhibitor. J Mol Cell Cardiol. 2018;115:73–81. doi: 10.1016/j.yjmcc.2017.12.015 [PubMed: 29294328]
51. Neef S, Mann C, Zwenger A, Dybkova N, Maier LS. Reduction of SR Ca(2+) leak and arrhythmogenic cellular correlates by SMP-114, a novel CaMKII inhibitor with oral bioavailability. Basic Res Cardiol. 2017;112:45. doi: 10.1007/s00395-017-0637-y [PubMed: 28612156]
52. Hegyi B, Chen-Izu Y, Jian Z, Shimkunas R, Izu LT, Banyasz T. KN-93 inhibits IKr in mammalian cardiomyocytes. J Mol Cell Cardiol. 2015;89:173–176. doi: 10.1016/j.yjmcc.2015.10.012 [PubMed: 26463508]
53. Zhang J, Liang R, Wang K, Zhang W, Zhang M, Jin L, Xie P, Zheng W, Shang H, Hu Q, et al. Novel CaMKII-delta Inhibitor Hesperadin Exerts Dual Functions to Ameliorate Cardiac Ischemia/Reperfusion Injury and Inhibit Tumor Growth. Circulation. 2022;145:1154–1168. doi: 10.1161/CIRCULATIONAHA.121.055920 [PubMed: 35317609]
54. Huang TP, Zhao KT, Miller SM, Gaudelli NM, Oakes BL, Fellmann C, Savage DF, Liu DR. Circularly permuted and PAM-modified Cas9 variants broaden the targeting scope of base editors. Nat Biotechnol. 2019;37:626–631. doi: 10.1038/s41587-019-0134-y [PubMed: 31110355]
55. Kluesner MG, Nedveck DA, Lahr WS, Garbe JR, Abrahante JE, Webber BR, Moriarity BS. EditR: A Method to Quantify Base Editing from Sanger Sequencing. CRISPR J. 2018;1:239–250. doi: 10.1089/crispr.2018.0014 [PubMed: 31021262]

56. Zhou Y, Zhou B, Pache L, Chang M, Khodabakhshi AH, Tanaseichuk O, Benner C, Chanda SK. Metascape provides a biologist-oriented resource for the analysis of systems-level datasets. Nat Commun. 2019;10:1523. doi: 10.1038/s41467-019-09234-6 [PubMed: 30944313]

57. Clement K, Rees H, Canver MC, Gehrke JM, Farouni R, Hsu JY, Cole MA, Liu DR, Joung JK, Bauer DE, et al. CRISPResso2 provides accurate and rapid genome editing sequence analysis. Nat Biotechnol. 2019;37:224–226. doi: 10.1038/s41587-019-0032-3 [PubMed: 30809026]

Clinical Perspective

What is new?

- The autophosphorylation site of CaMKIIδ can be ablated by CRISPR-Cas9 adenine base editing.
- Rendering CaMKIIδ phospho-resistant improves cardiac function and confers protection from heart failure-related mortality and pathological remodeling.

What are the clinical implications?

- We identified an adenine base editing strategy with a sgRNA that is applicable for the human and mouse genome.
- Base editing has a specificity of >2,000-fold toward *CaMKIIδ*, which is an important safety feature.
- The autophosphorylation site of CaMKIIδ is a promising therapeutic target for cardiac disorders.

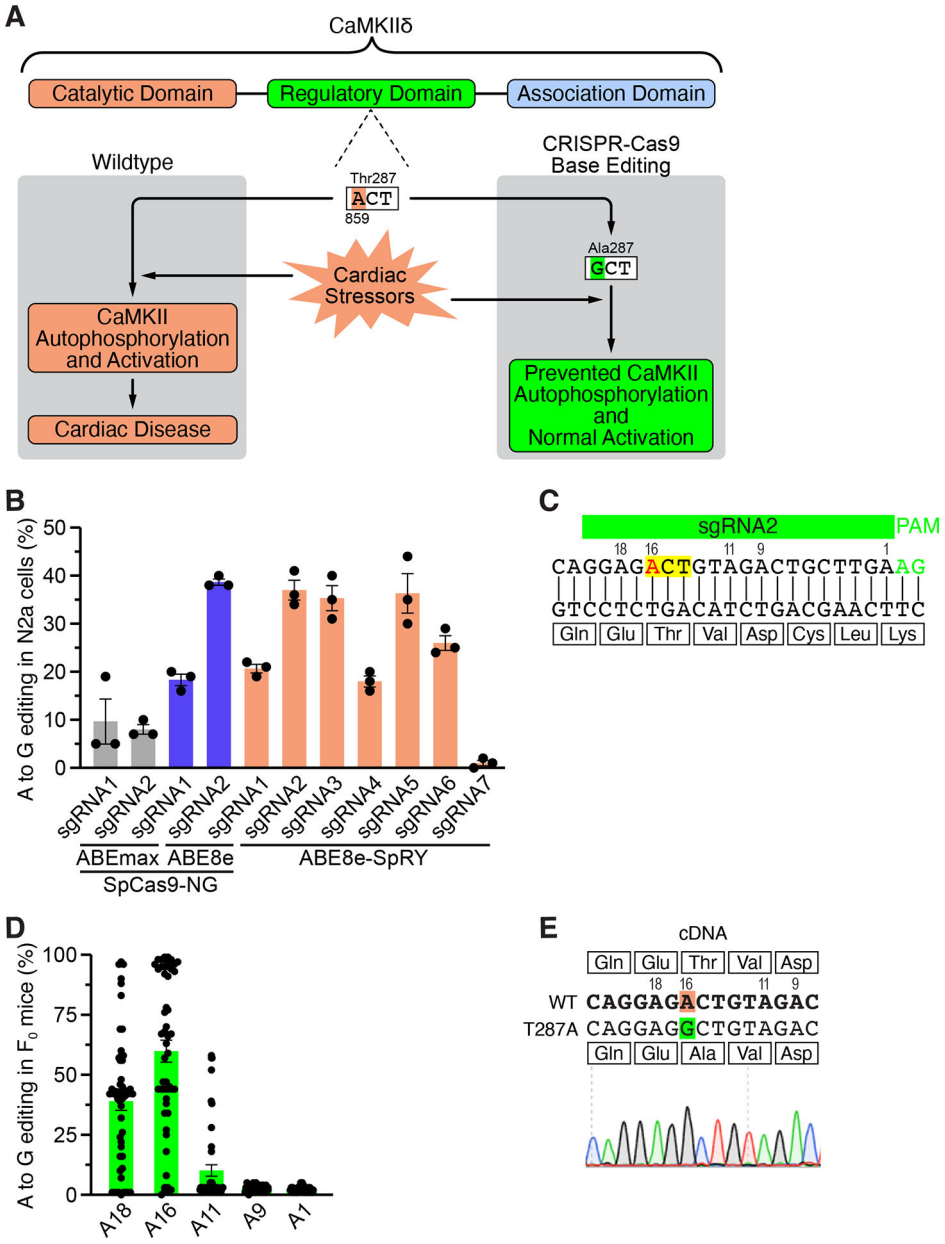

Figure 1. Adenine base editing to ablate the autophosphorylation site of CaMKIIδ.

A, Overview of CaMKIIδ with its three domains. Autophosphorylation occurs at threonine-287 in the regulatory domain. Several cardiac stressors have been shown to promote CaMKIIδ autophosphorylation and hyperactivation, subsequently leading to cardiac disease. Using CRISPR-Cas9 adenine base editing, we discovered a strategy to edit c.A859G (p.T287A), thereby ablating the autophosphorylation site of CaMKIIδ. **B,** Percentage of adenine (A) to guanine (G) editing in mouse N2a cells at c.A859 (p.T287) for sgRNAs 1–7 combined with either ABEmax or ABE8e that were fused to either SpCas9-NG or SpRY (n=3 transfections). **C,** DNA sequence showing a segment of the mouse *CaMKIIδ* gene encoding part of the regulatory domain with alignment of sgRNA2 that has 100% homology to that region. The PAM sequence is in green and the ACT nucleotide triplet encoding the

critical threonine-287 is highlighted in yellow. Each adenine along the sequence of sgRNA2 is numbered (counting from the PAM). **D,** Percentage of adenine (A) to guanine (G) editing in F_0 mice (n=52) for each adenine in sgRNA2 following injection of sgRNA2 and ABE8e fused to SpCas9-NG in zygotes and subsequent transfer into the oviducts of pseudo-pregnant female mice. **E,** Sequencing of cDNA of a homozygous T287A mouse showing the single nucleotide edit c.A859G that makes CaMKIIδ phospho-resistant. Data are presented as individual data points with mean ± SEM and replicates are either independent transfections (B) or individual mice (D).

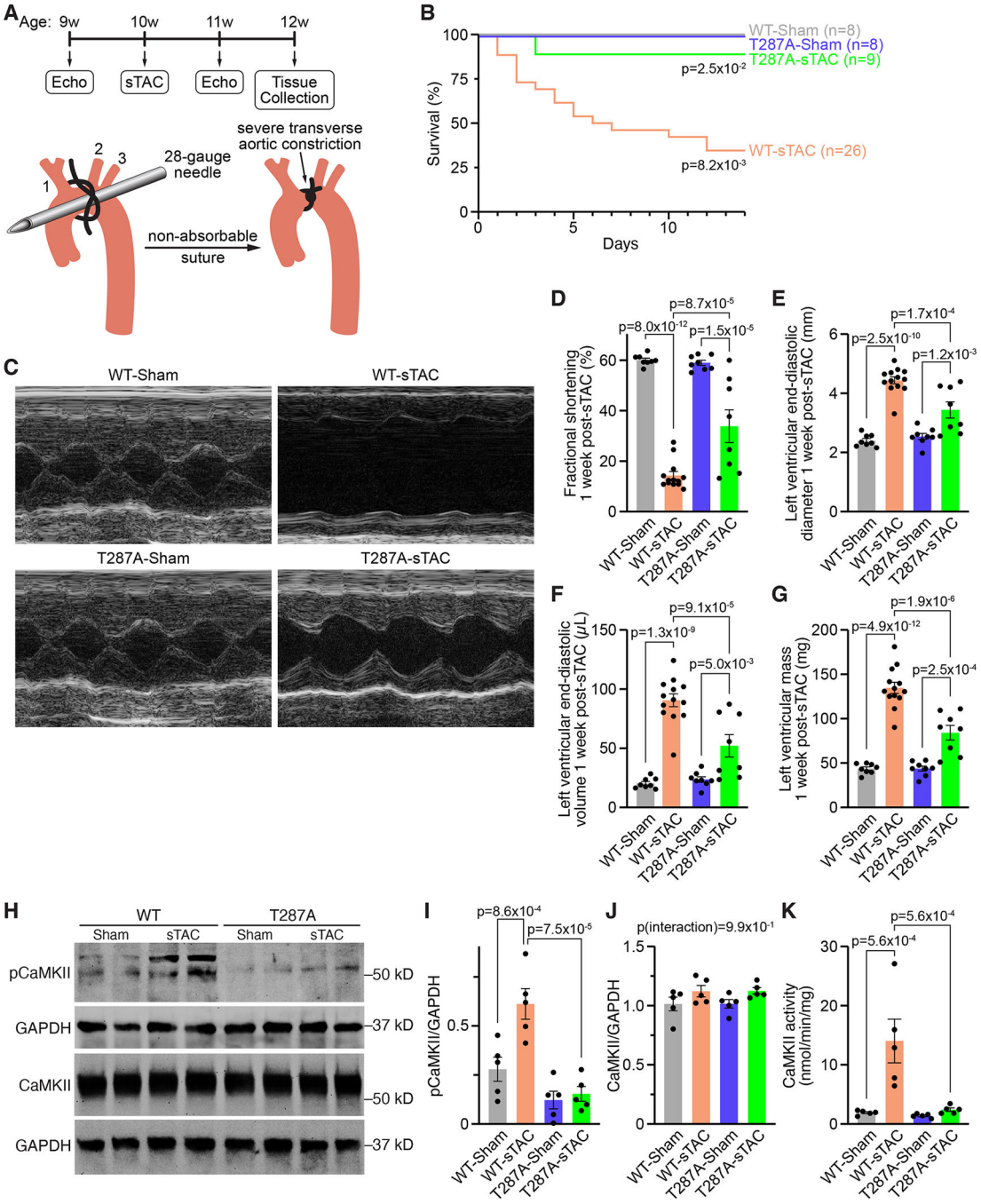

Figure 2. Ablation of CaMKIIδ autophosphorylation improves survival and cardiac function post-sTAC.

A, Experimental design for subjecting male mice at 10 weeks of age to sTAC surgery as a model for afterload-induced heart failure. Cardiac function was assessed by echocardiography one week before and one week after sTAC. Two weeks after sTAC, mice were sacrificed, and hearts harvested for further histological and molecular analyses (1 – brachiocephalic artery, 2 – left common carotid artery, 3 – left subclavian artery). **B,** Survival curves of WT-Sham, WT-sTAC, T287A-Sham, and T287A-sTAC mice

($p=8.2\times10^{-3}$ for WT-sTAC vs. WT-Sham, $p=2.5\times10^{-2}$ for T287A-sTAC vs. WT-sTAC). **C,** Representative M-mode recordings of mouse hearts from all groups 1-week post-sTAC/Sham surgery, as acquired by echocardiography. **D,** Mean fractional shortening. **E,** Mean left ventricular end-diastolic diameter. **F,** Mean left ventricular end-diastolic volume. **G,** Mean left ventricular mass. **H,** Western blot analysis of autophosphorylated CaMKII and total CaMKII (each with GAPDH as housekeeper protein) for all groups. **I,** Mean densitometric analyses for autophosphorylated CaMKII normalized to GAPDH for all groups. **J,** Mean densitometric analyses for total CaMKII normalized to GAPDH for all groups. **K,** Mean CaMKII activity for all groups. Data are presented as individual data points with mean ± SEM and all replicates are individual mice. Statistical comparisons are based on log-rank (Mantel-Cox) test with Bonferroni's post-hoc correction (B) and on two-way ANOVA post-hoc corrected by Holm-Sidak (D-G,I-K).

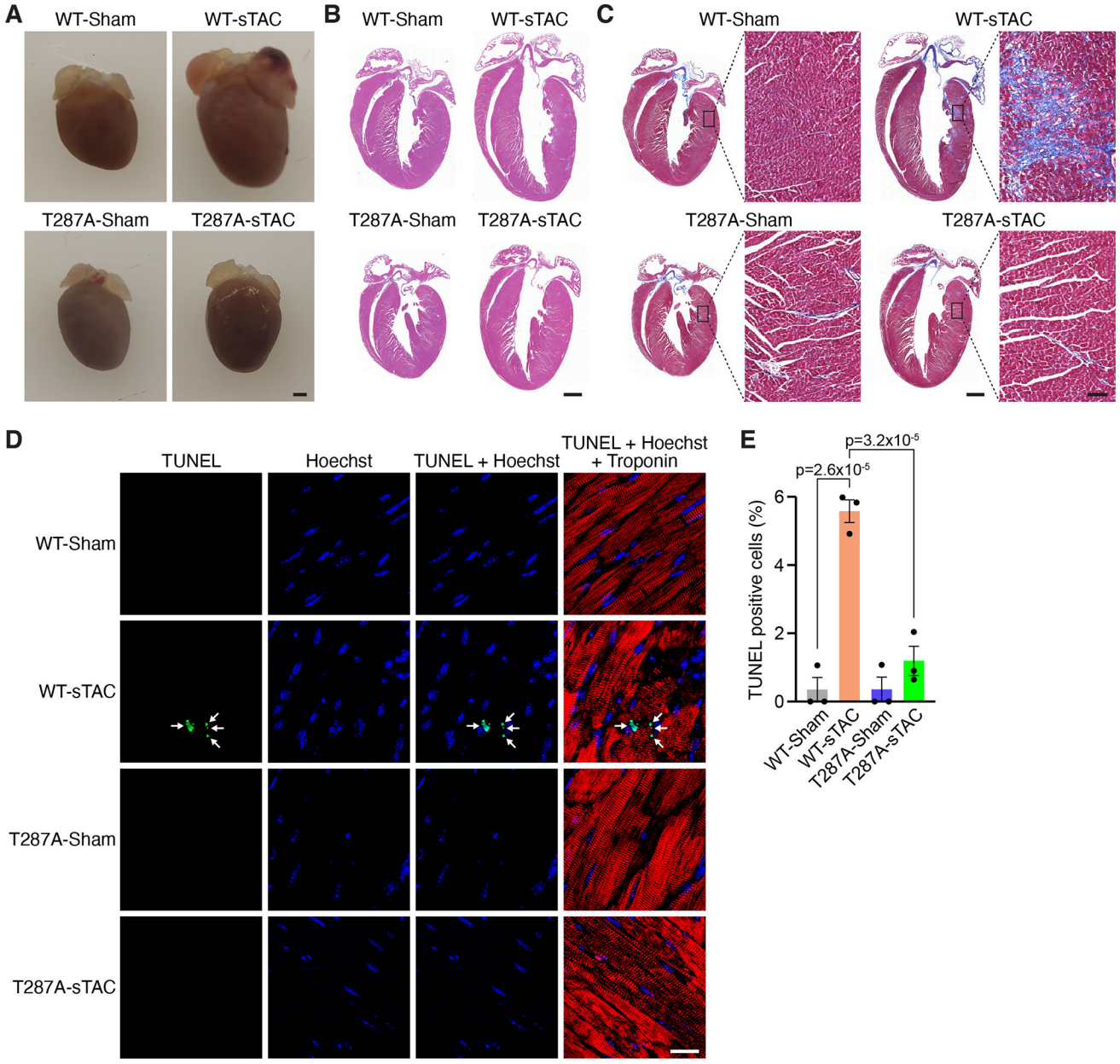

Figure 3. Rendering CaMKIIδ phospho-resistant prevents myocardial fibrosis and apoptosis.

A, Macroscopic images of hearts from WT-Sham, WT-sTAC, T287A-Sham, and T287A-sTAC mice (scale bar 1 mm). **B,** H&E staining of cardiac sections for each group (scale bar 1 mm). **C,** Trichrome staining of cardiac sections for each group (scale bar 1 mm for whole hearts and 100 μm for close-ups). **D,** Representative heart sections for all groups showing immunohistochemistry of TUNEL (green, arrows), Hoechst 33342 (blue, for nuclei), and cardiac troponin (red; scale bar 20 μm). **E,** Mean percentage of apoptotic cells for each group. Data are presented as individual data points with mean ± SEM and all replicates are individual mice. Statistical comparisons are based on two-way ANOVA post-hoc corrected by Holm-Sidak.

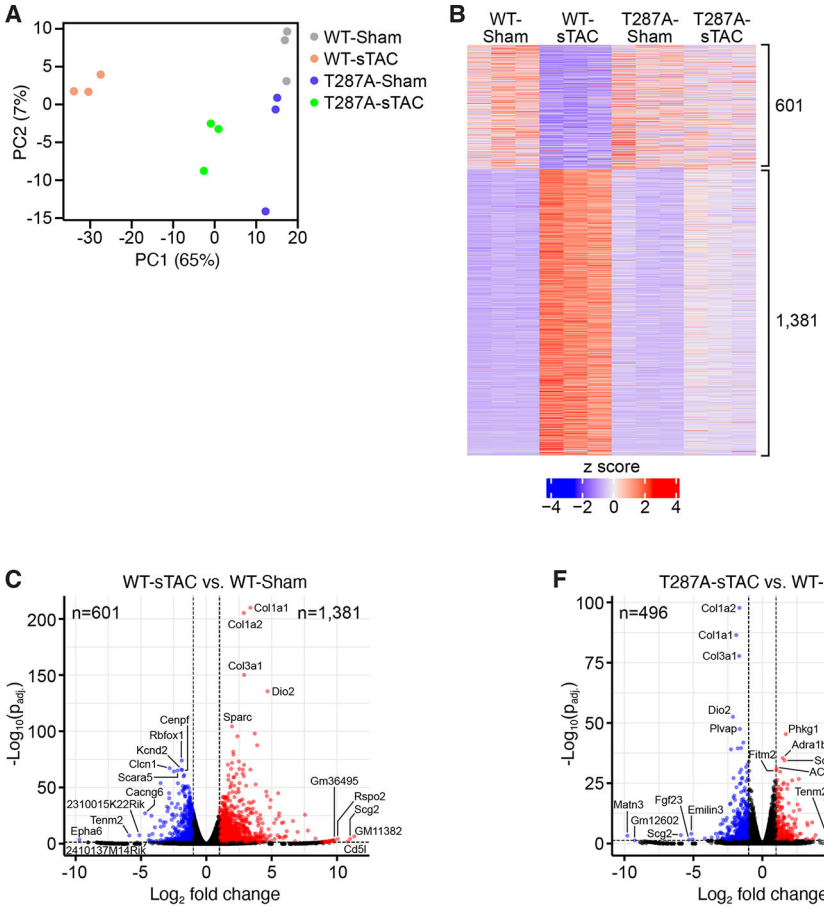

D

GO pathways of upregulated genes in WT-sTAC vs. WT-Sham	-Log10(p)
Extracellular matrix organization	38.9
Mitotic cell cycle process	27.4
Positive regulation of response to external stimulus	24.9
Inflammatory response	24.2
Leukocyte migration	18.1
Leukocyte activation	17.8
Supramolecular fiber organization	17.7
Regulation of vasculature development	15.9

G

GO pathways of upregulated genes in T287A-sTAC vs. WT-sTAC	-Log10(p)
Monoatomic ion transmembrane transport	8.5
Fatty acid metabolic process	7.0
Lipid localization	5.5
Acyl-CoA metabolic process	5.3
Muscle system process	5.0
Regulation of muscle contraction	5.0
Cellular carbohydrate metabolic process	4.5
Calcium ion transmembrane transport	2.4

E

GO pathways of downregulated genes in WT-sTAC vs. WT-Sham	-Log10(p)
Fatty acid metabolic process	14.1
Monoatomic ion transmembrane transport	12.1
Regulation of heart contraction	9.3
Acyl-CoA metabolic process	8.1
Muscle system process	7.9
Lipid localization	6.2
Regulation of cardiac muscle contraction by calcium ion signaling	2.6
Calcium ion transport	2.0

H

GO pathways of downregulated genes in T287A-sTAC vs. WT-sTAC	-Log10(p)
Extracellular matrix organization	28.5
Mitotic cell cycle process	14.9
Vasculature development	12.6
Positive regulation of response to external stimulus	12.0
Inflammatory response	10.7
Leukocyte migration	9.1
Collagen metabolic process	8.4
Tissue remodeling	8.3

Figure 4. Ablation of CaMKIIδ autophosphorylation protects mice from dysregulation of the cardiac transcriptome.

A, Principal component analysis (PCA) of the cardiac transcriptome of WT and T287A mice, both subjected to sham and sTAC surgery (n=3 per group). **B,** Heat map of 1,982 genes that were differentially expressed between WT-sTAC compared to WT-Sham by more than 2-fold. Additionally, we are reporting the same genes for T287A-Sham and T287A-sTAC. **C,** Volcano plot showing 1,381 and 601 genes that were up- and downregulated, respectively, by at least 2-fold in WT-sTAC compared to WT-Sham mice. The top 5 up- and

downregulated genes are labeled, based on both p-value and fold change. **D,** Gene Ontology terms associated with upregulated genes in WT-sTAC compared to WT-Sham mice. **E,** Gene Ontology terms associated with downregulated genes in WT-sTAC compared to WT-Sham mice. **F,** Volcano plot showing 264 and 496 genes that were up- and downregulated, respectively, by at least 2-fold in T287A-sTAC compared to WT-sTAC mice. The top 5 up- and downregulated genes are labeled, based on both p-value and fold change. **G,** Gene Ontology terms associated with upregulated genes in T287A-sTAC compared to WT-sTAC mice. **H,** Gene Ontology terms associated with downregulated genes in T287A-sTAC compared to WT-sTAC mice. Data are presented as individual data points and all replicates are individual mice.

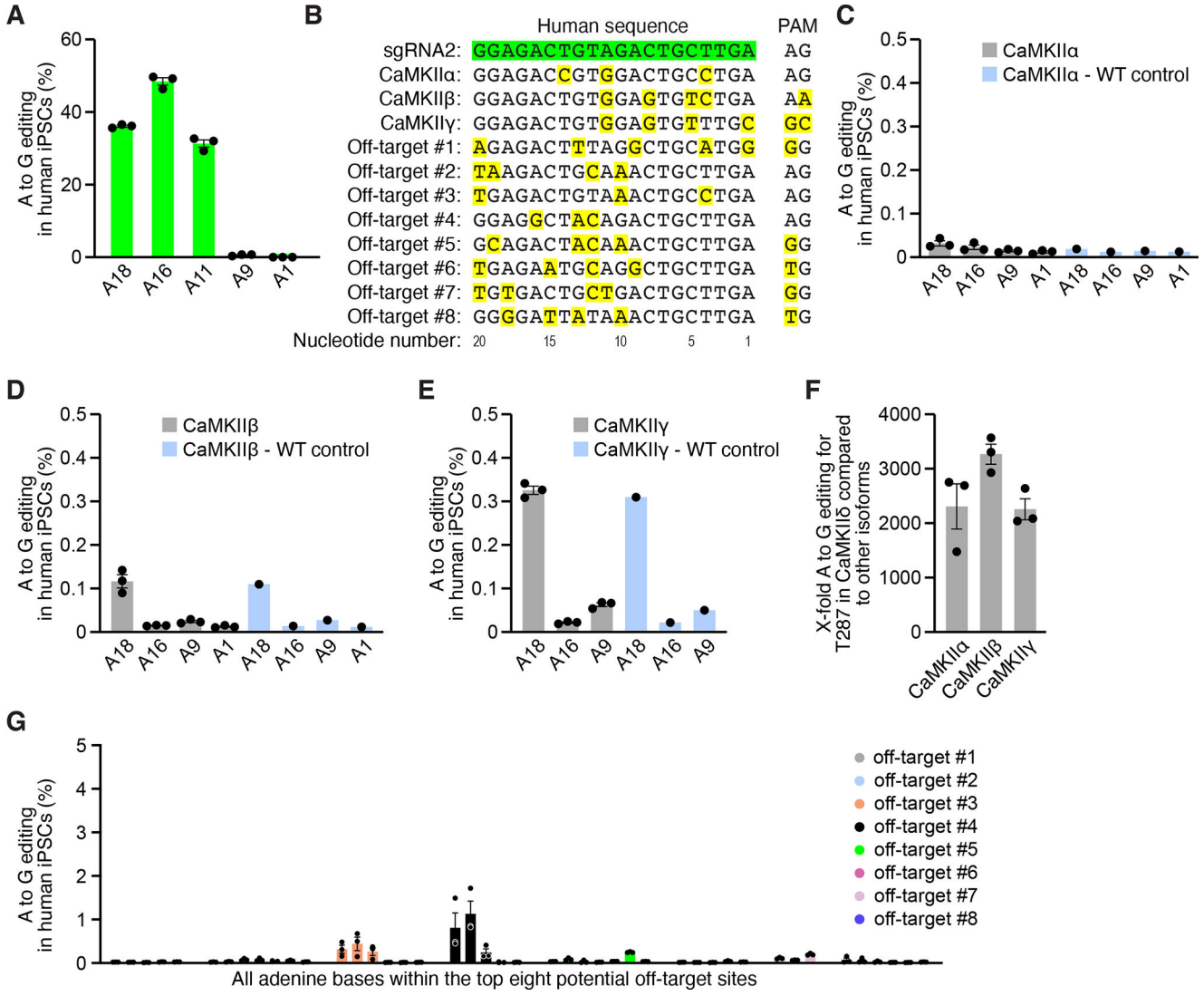

Figure 5. Analysis of *CaMKIIδ* editing and potential off-targets in human iPSCs using deep amplicon sequencing.

A, Percentage of adenine (A) to guanine (G) editing for each adenine in sgRNA2 (*CaMKIIδ*) following base editing with sgRNA2 and ABE8e. **B,** Sequence of sgRNA2 (*CaMKIIδ*) and the corresponding DNA and PAM sequences of *CaMKIIα*, *β*, and *γ* as well as the sequences of the top 8 potential off-target loci, as predicted by CRISPOR. Yellow highlighting indicates bases different from sgRNA2. Each nucleotide within the sequence is numbered (counting from the PAM). **C,** Percentage of adenine (A) to guanine (G) editing for all adenines within the DNA sequence of *CaMKIIα* corresponding to sgRNA2, either following base editing with sgRNA2 and ABE8e or for an untreated human WT sample (WT control). **D,** Percentage of adenine (A) to guanine (G) editing for all adenines within the DNA sequence of *CaMKIIβ* corresponding to sgRNA2, either following base editing with sgRNA2 and ABE8e or for an untreated human WT sample (WT control). **E,** Percentage of adenine (A) to guanine (G) editing for all adenines within the DNA sequence of *CaMKIIγ* corresponding to sgRNA2, either following base editing with sgRNA2 and

ABE8e or for an untreated human WT sample (WT control). **F,** Fold change of percentage of adenine (A) to guanine (G) editing at c.A859G (p.T287A) for *CaMKIIδ* compared to *CaMKIIα*, *β*, and *γ*. **G,** Percentage of adenine (A) to guanine (G) editing for all adenines (ordered from 5' to 3') within the DNA sequences of the top 8 predicted off-target loci, beginning with the potential off-target #1. Data are presented as individual data points with mean ± SEM and all replicates are human iPSCs following three independent nucleofections with sgRNA2 and ABE8e fused to SpCas9-NG. As a negative control, we analyzed one human WT iPSC sample that was not treated with sgRNA2 and ABE8e fused to SpCas9-NG (WT control).

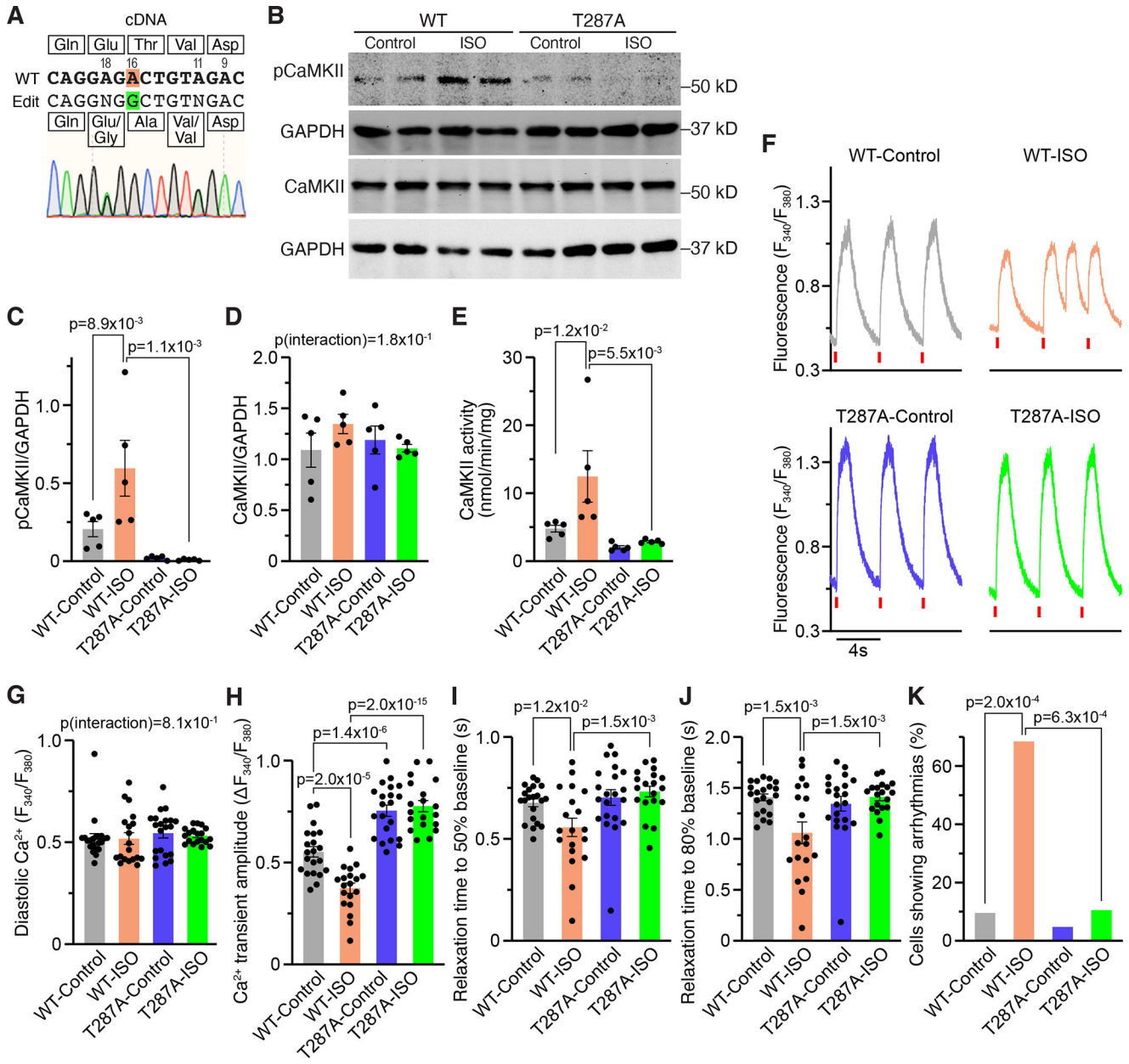

Figure 6. ABE with sgRNA2 protects human iPSC-CMs from ISO-induced dysregulation of cellular Ca^{2+} homeostasis.

A, Sequencing of cDNA of human iPSC-CMs showing the editing pattern of sgRNA2. **B,** Western blot analysis of autophosphorylated CaMKII and total CaMKII (each with GAPDH as housekeeper protein) in human wildtype (WT) and T287A iPSC-CMs for both control and 10 days of exposure to isoproterenol (ISO). **C,** Mean densitometric analysis for autophosphorylated CaMKII normalized to GAPDH. **D,** Mean densitometric analysis for total CaMKII normalized to GAPDH. **E,** Mean CaMKII activity in WT and T287A iPSC-CMs both upon control and ISO. **F,** Representative Ca^{2+} transients for WT and T287A human iPSC-CMs upon control and 10 days of chronic ISO, measured by epifluorescence microscopy. **G,** Mean diastolic Ca^{2+} levels for all groups. **H,** Mean Ca^{2+} transient amplitude

for each group. **I,** Mean relaxation time to 50% baseline. **J,** Mean relaxation time to 80% baseline. **K,** Percentage of iPSC-CMs showing arrhythmias. Data are presented as individual data points with mean ± SEM and all replicates are either 5 independent differentiations into iPSC-CMs (C-E) or individual iPSC-CMs (G-K). Statistical comparisons were performed with two-way ANOVA post-hoc corrected by Holm-Sidak (C-E,G-J) and with Fisher's exact test (K).